

OPTIMAL CONTROL OF HELICOPTER VIBRATION THROUGH CYCLIC VARIATIONS IN BLADE ROOT STIFFNESS

Phuriwat Anusonti-Inthra* and Farhan Gandhi**

Rotorcraft Center of Excellence
Department of Aerospace Engineering
The Pennsylvania State University
233 Hammond Building, University Park, PA 16802

Abstract

The study demonstrates that optimal multi-cyclic variations of blade root flap and lag stiffness can produce simultaneous reductions in all components of vibratory hub loads of a 4-bladed hingeless rotor helicopter. Both gradient and non-gradient based optimization schemes are successful in reducing the hub vibrations. The required stiffness variations can be reduced (without significantly compromising performance) by introducing a penalty on the input in the objective function used for minimization. Reductions in the vibration performance index of over 90% were seen with optimal $2/rev$ and $3/rev$ flap and lag stiffness variations. The concept was effective in reducing vibration over a range of variations in configuration (fundamental flap, lag, and torsion frequencies) and operational parameters (forward speed). Further, it was shown that stiffness variations of *discrete flap and lag springs* introduced in the blade root region are effective in reducing vibratory hub loads. Thus, introduction of discrete controllable stiffness elements (devices) is a viable method for practically varying stiffness of the blade root region.

1. Introduction

In forward flight, helicopters can experience severe vibration due to the rotor blades operating in a periodic aerodynamic environment. These vibrations result in significant crew and passenger discomfort, increased component fatigue and maintenance requirements, and reduced effectiveness of weapon systems for military helicopters. Accordingly, considerable effort has been devoted over the past decades to examine passive design and active control strategies for helicopter vibration reduction (see for example Refs. 1-10).

Common techniques for passive vibration reduction include use of vibration absorbers, isolators, and structural and aerodynamic design optimization of the rotor blades. While these concepts produce some vibration reduction in certain flight conditions, they generally involve a significant weight penalty and constitute a fixed design (inability to adapt to changes in conditions). Active vibration reduction strategies including Higher Harmonic Control (HHC), Individual Blade Control (IBC), and Active Control of Structural Response (ACSR) have also been examined extensively. HHC or IBC involves actively controlling the blade pitch or trailing edge flap deflections so as to generate unsteady higher harmonic aerodynamic loads that cancel the original vibration. Although these methods can be effective, they usually

involve high power requirements, added weight and complexity, and high pitch-link loads. Further, IBC requires use of slip rings capable of transferring enough power to the actuators in the rotating frame. ACSR uses actuators carefully located in the airframe to actively cancel the incoming N/rev vibration from the rotor. While this method can locally reduce airframe vibration, the high vibration levels and dynamic stresses experienced by the rotor blades remain unaltered.

Recently a new semi-active approach was proposed for helicopter vibration reduction [11], involving cyclic variation of the effective flap, lag, and torsion stiffness of the blade root region. It was shown that by introducing small-to-moderate amplitude stiffness variations at harmonics of the rotor speed, considerable reduction in vibratory hub loads was possible [11]. A semi-active approach defers from purely active approaches to rotor control (HHC and IBC) in that large aerodynamic forces do not have to be overcome in every cycle (a requirement with pure active approaches involving twisting of the blade, changing of the blade pitch, or deflection of a trailing edge flap device). Consequently, power requirements for semi-active control schemes tend to be significantly smaller for comparable performance; and such strategies have already been widely explored for vibration reduction applications in civil structures [12-15] and automobile suspension [16-19]. An additional

* Graduate Research Assistant

** Assistant Professor and corresponding author (e-mail: fgandhi@psu.edu, Tel: 814-865-1164, Fax: 814-865-7092)
Proceedings of the 26th European Rotorcraft Forum, Sept. 26-29, 2000, The Hague, The Netherlands

advantage of semi-active control is that unlike pure active control, no energy is being pumped into the controlled system, so no potential for instability is introduced. While both semi-active as well as pure active rotor control favorably modify the rotor blade response in reducing vibration, a semi-active approach achieves this by modulating the system properties whereas pure active control generates forces and moments on the blade. In practice, stiffness variations of the blade root region could be achieved by introducing discrete devices such as controllable orifice devices [20] or controllable Magnetorheological (MR) fluid based devices in the blade root region [21, 22]. Through parametric studies, Ref. 11 clearly established the sensitivity of hub vibrations to individual cyclic stiffness variations and explained, in detail, the underlying physical mechanisms by which vibration reductions were achieved. However, an optimal controller using multi-cyclic stiffness variations, that simultaneously reduced all six components of vibratory hub loads, was not developed.

2. Focus of the Present Study

In Ref. 11 it was shown that $2/rev$ and $3/rev$ flap and lag stiffness variations are most effective for reducing the $4/rev$ hub vibrations of a 4-bladed hingeless rotor helicopter. The primary focus of the present study is to develop an optimal multi-cyclic controller that determines the amplitudes and phase values of these stiffness variation inputs for simultaneous minimization of all components of vibratory hub loads. Both gradient and non-gradient based optimization schemes are used to minimize a quadratic objective function comprising of all components of $4/rev$ hub vibrations, with the latter guaranteed to yield a *global minima* of the objective function. The effect of introducing a penalty on the input is examined, as well, to limit the magnitude of the stiffness variations required.

The effectiveness of the multi-cyclic controller is evaluated for variations in rotor parameters such as fundamental flap, lag, and torsion frequencies; as well as variations in operating condition (cruise speed). In addition to overall stiffness variations of the root element of the rotor blade, effectiveness of cyclic variations in the stiffness of *discrete flap and lag springs* introduced in the blade root region is examined as well. Although these discrete springs represent unspecified (generic) variable stiffness devices, it clearly demonstrates that such discrete devices would indeed be effective in reducing vibratory hub loads of a helicopter.

3. Analysis Method

To evaluate the effectiveness of optimal cyclic stiffness variations for helicopter hub vibration

reduction, a comprehensive rotorcraft aeroelastic analysis based on the UMARC formulation [23] is used. A BO-105 type 4-bladed hingeless rotor helicopter is simulated, with the blades assumed to undergo elastic flap- and lag-bending, and elastic torsion deformations. The sectional aerodynamic loads are calculated using blade element theory, with the inflow calculated using the Drees model. In the analysis, the blades are spatially discretized using the Finite Element Method, and the discretized blade equations of motion are transformed to modal space to reduce computational cost. Blade periodic response in forward flight is calculated using the temporal finite element method. Evaluation of blade response and vehicle equilibrium (vehicle orientation and controls) is carried out iteratively in a coupled response-trim calculation procedure. Such a coupled solution procedure is required since the blade response influences the steady hub forces and moments, which impact the vehicle orientation and control settings. These, in turn, affect the blade response. The converged solution yields the vehicle orientation and controls, blade periodic response, as well as the vibratory blade root loads and hub loads.

The spatial discretization of the rotor blade is shown in Fig. 1, and the flap and lag stiffness (EI_β and EI_ζ , respectively) of the root element is varied cyclically as follows:

$$EI_\beta(\psi) = \overline{EI}_\beta + \sum_{i=1}^n [\Delta EI_\beta^{np} \sin(n\psi + \phi_n^\beta)] \quad (1a)$$

$$EI_\zeta(\psi) = \overline{EI}_\zeta + \sum_{i=1}^n [\Delta EI_\zeta^{np} \sin(n\psi + \phi_n^\zeta)] \quad (1b)$$

In the above equations, “ n ” represents the frequency of the stiffness variations ($n=1$ implies $1/rev$ variations in stiffness, $n=2$ implies $2/rev$ variations, etc); and “ ϕ_n ” represents the phase angle of the stiffness variation at n/rev . The amplitudes of stiffness variations, ΔEI_β and ΔEI_ζ , are expressed as percentages of their baseline values (\overline{EI}_β and \overline{EI}_ζ , respectively). Equations 1 can be written in a compact form as:

$$K(\psi) = \overline{K} + \sum_{i=1}^n [\Delta K^{np} \sin(n\psi + \phi_n)] \quad (2)$$

The coupled blade flap-lag-torsion equations of motion can then be written symbolically as,

$$M^* q + C^* q + \{K + \Delta K(\psi)\} q = F^{NL}$$

$$\text{or} \quad M^* q + C^* q + K q = F^{NL} - \Delta K(\psi) q \quad (3)$$

where F^{NL} includes all the constant as well as nonlinear elastic, inertial, and aerodynamic contributions. Clearly, the $\Delta K(\psi) q$ term (due to stiffness variation) can be regarded as an unsteady loading that, in essence, can be used to modify the

blade response as desired. Traditional HHC or IBC is based on the generation of unsteady forces (of aerodynamic origin) at $3/rev$, $4/rev$, and $5/rev$. In the present concept, since the blade periodic response, q , itself contains harmonics of rotor frequency, lower harmonic variations of stiffness, $\Delta K(\psi)$, would also be able to generate unsteady loads, $\Delta K(\psi)q$, at $3/rev$, $4/rev$, and $5/rev$, for a 4-bladed rotor.

To determine the optimal stiffness variation, $\Delta K(\psi)$, the approach used is similar to that employed in previous active vibration reduction studies [24]. Instead of the active control (blade pitch or trailing edge flap) inputs, it is assumed that the stiffness variations, ΔK , relate to the helicopter vibration output, z , through a transfer function, T , as follows:

$$z_n = z_o + T \Delta K_n \quad (4)$$

Where “ z_o ” represents the baseline $4/rev$ hub vibration, while “ z_n ” represents $4/rev$ hub vibration in the presence of variation in stiffness, ΔK_n . The transfer function, T , is numerically calculated by perturbation of individual stiffness components, about the baseline configuration.

The control algorithm, adapted from Ref. 24, is in general based on the minimization of a composite quadratic objective function, J , defined as:

$$J = J_z + J_k = z_n^T W_z z_n + \Delta K_n^T W_k \Delta K_n \quad (5)$$

where “ W_z ” represents the weighting on output vibration, and “ W_k ” represents the penalty weighting on input.

Gradient and non-gradient based methods are used to minimize J and determine the optimal input (stiffness variation). In the gradient based method, an optimal solution can be found by substituting Eq. (4) into Eq. (5) and setting $\partial J / \partial \Delta K_n = 0$. The resulting optimal input is:

$$\Delta K_n = -(T^T W_z T + W_k)^{-1} T^T W_z z_o \quad (6)$$

The non-gradient optimization method considered is based on a Genetic Algorithm (GA) approach [25]. An optimal input is determined through an evolutionary process replicating natural selection. Any possible input is coded into a binary string called an individual. Each individual has a fitness that corresponds to its performance index. The most “fit” individuals produce the next generation through a mating and mutation process. After several generations, the process will produce the individual with the highest fitness that represents the optimal solution. For the genetic algorithm simulations conducted in the present study, the following parameters are considered - variable size of 2-8,

number of individuals in each generation is 20; and number of generations is 50-200.

In the optimization studies of the following sections, J_z (which is a measure of the vibration level) is used as a vibration performance index; with smaller values of J_z indicating more vibration reduction due to cyclic stiffness variation.

In practice, it is anticipated that root stiffness variation will be achieved through discrete controllable stiffness devices introduced in the root region of the blade (see schematic sketch, Fig. 2). These devices could be expected to contribute significantly to the baseline rotor stiffness and can be mathematically represented by introducing the controllable springs K_w , $K_{w'}$, K_v , and $K_{v'}$ (as shown in Fig. 2). However, it should be noted that since a single device contributes to both the translational and rotational flap stiffness, K_w and $K_{w'}$ are not independent. Similarly, K_v and $K_{v'}$ are due to the same device and are again not independent. The ratio of the translational to rotational stiffness depends on the device configuration and is a known constant. Cyclic variations in these spring stiffnesses are then represented as follows:

$$\begin{aligned} K_w(\psi) &= \bar{K}_w + \sum_{i=1}^n [\Delta K_w^{np} \sin(n\psi + \phi_n^w)] \\ K_{w'}(\psi) &= \alpha_w \bar{K}_w + \sum_{i=1}^n [\alpha_w \Delta K_w^{np} \sin(n\psi + \phi_n^w)] \\ K_v(\psi) &= \bar{K}_v + \sum_{i=1}^n [\Delta K_v^{np} \sin(n\psi + \phi_n^v)] \\ K_{v'}(\psi) &= \alpha_v \bar{K}_v + \sum_{i=1}^n [\alpha_v \Delta K_v^{np} \sin(n\psi + \phi_n^v)] \end{aligned} \quad (7)$$

where \bar{K}_w , \bar{K}_v , α_w and α_v are known constants. These stiffness variations of a discrete device would effectively produce the overall stiffness variations of the blade root region required for hub vibration reduction. Results provided in section 4.6 demonstrate that optimal variations of discrete spring stiffness do indeed produce hub vibration reductions.

4. Results and Discussion

The effect of the optimal cyclic variations in blade root stiffness on hub vibration reduction is first examined at an advance ratio of 0.3 and a thrust level corresponding to $C_T/\sigma = 0.07$, for a baseline configuration (BO-105 type 4-bladed hingeless rotor helicopter) whose rotor-fuselage properties are given in Table 1. Without any cyclic stiffness variation, the predicted vibratory hub loads and blade root loads for the baseline configuration (at advance ratio 0.3) are given in Table 2. The performance of a series of optimal controllers using $3/rev$ flap stiffness variation,

2-3/rev flap and 3/rev lag stiffness variations, and 2-3/rev flap and lag stiffness variations, respectively, are examined in Sections 4.1 – 4.3. Both gradient and non-gradient based optimization methods are used and the effect of introducing penalty on input controls is examined as well. Sections 4.4 and 4.5, respectively, evaluate the effectiveness of the control scheme for variations in baseline configuration and cruise speed. Finally, Section 4.6 demonstrates the effectiveness of discrete controllable stiffness devices in reducing vibratory hub loads.

4.1 Optimal 3/rev flap stiffness variation

Using gradient-based optimization, the 3/rev flap stiffness variation is determined that minimizes an objective function comprising of all components of vibratory hub loads (with no penalty on input; $J = J_z$, $W_k = 0$). The amplitude of the optimal 3/rev flap stiffness variation was found to be $\Delta EI_\beta^{3p} = 10.75\%$ of the baseline flap stiffness, \overline{EI}_β , and the phase, $\phi = 22.5^\circ$. Fig. 3 shows contours corresponding to constant values of the objective function versus cosine and sine components of the 3/rev flap stiffness variations. It is seen that the optimal solution yields a 65% reduction in objective function, and the corresponding reductions in individual components of vibratory hub loads are shown in Fig 4. From the figure it is seen that 40-60% reductions in the in-plane hub forces and moments, and 25-30% reductions in the vertical shear and hub torque are simultaneously achieved. Corresponding to the optimal 3/rev flap stiffness variation, the harmonics of blade root loads are calculated and summarized in Table 3. Small percentage increases in S_r^{4p} and M_β^{4p} , and larger percentage increases in S_z^{5p} and M_β^{5p} are observed. However, it should be noted that the baseline values for the 5th harmonic of all components of blade root loads are extremely small (see Table 2b).

4.2 Optimal 2,3/rev flap & 3/rev lag stiffness variations

Next, 2/rev and 3/rev flap stiffness variation and 3/rev lag stiffness variation is simultaneously considered for vibration reduction. Using a gradient-based minimization of an objective function comprising of the components of vibratory hub loads ($J = J_z$, $W_k = 0$), the optimal solution (stiffness variations) are shown in Table 4. For these optimal stiffness variations, the performance index, J_z , is reduced by a significant 91% (compared to the baseline). The reductions in individual components of vibratory hub loads are shown in Fig. 5 (55-65% reductions in F_x^{4p} and F_y^{4p} , a 70% reduction in F_z^{4p} , 75-80% reductions in M_x^{4p} and M_y^{4p} , and a 90% reduction in M_z^{4p} are observed). As expected, these reductions are significantly larger than those obtained using optimal 3/rev flap stiffness variations alone. However a large 2/rev flap stiffness variation was required (Table 4).

4.3 Optimal 2,3/rev flap & lag stiffness variations

Vibration reductions achieved with optimal 2/rev and 3/rev flap, and 2/rev and 3/rev lag stiffness variations are presented in Fig. 6. The figure includes results obtained using both gradient (G) and non-gradient (NG) based methods to minimize an objective function comprising of the components of vibratory hub loads ($J = J_z$, $W_k = 0$); and the corresponding optimal control inputs are shown in Table 5. Overall, the vibration reductions obtained are slightly larger than the corresponding reductions in the previous section without 2/rev lag stiffness variations (compare Fig. 5 to the results in Fig. 6 corresponding to gradient based optimization; and note also that J_z is reduced from 8.92% in Table 4 to 7.34% in Table 5). From Table 5 it is seen that a nongradient based optimization yields a different solution (different optimal stiffness variations) from that obtained through gradient-based optimization, with larger overall vibration reduction (evident from the lower value attained by the objective function or performance index, J_z). This suggests that the gradient-based optimization located a local-minimum (as opposed to the global-minimum located using the NG-based approach). However, due to the nature of the non-gradient based optimization (stochastic optimization), the calculation time used is much longer than that of the gradient-based optimization. Both gradient as well as non-gradient based solutions yield large 2/rev flap stiffness variation, and the gradient-based approach further requires large 2/rev lag stiffness variation.

Due to large stiffness variations (2/rev variations) required, the objective function is extended to include a penalty weighting on the input controls ($W_k = I$). As a result, the optimal stiffness variations are reduced significantly (Table 6), without any significant adverse effect on the performance (see Fig. 7). Penalty on the input controls reduced the optimal ΔEI_ξ^{2p} from 31% to 15% of the baseline lag stiffness (the vibration performance index was virtually unchanged). For many other cases similar results were obtained – significant reductions in required stiffness variations for relatively small reductions performance, due to introduction of penalty on control inputs ($W_k = I$). For the optimal stiffness variations of Table 6 with penalty on the input controls, the changes in harmonics of blade root loads (compared to the baseline) are summarized in Table 7. Although large percentage increases are seen in M_ϕ^{4p} , and most of the 5/rev components of blade root loads, the baseline values for harmonics of the blade root pitching moment, and the 5/rev components of all root loads are very small (Table 2b).

4.4 Influence of baseline stiffness on effectiveness of vibration control

Sections 4.1-4.3 established the effectiveness of multi-cyclic variations in flap and lag stiffness for reduction of vibrations of the baseline configuration whose properties are given in Table 1. The present section examines the effectiveness of the proposed concept for configuration variations. Specifically, the rotor flap, lag, and torsion stiffness (and correspondingly, the flap, lag, and torsion frequencies) are individually varied, and the effectiveness of cyclic stiffness variations to reduce vibration are re-examined.

Figure 8 shows the hub vibration index, J_z , for variation in fundamental flap frequency. As the blade baseline flap stiffness, \overline{EI}_β , (and flap frequency) decreases, the vibration index (without cyclic stiffness variation) initially increases by 30% but then decreases once the first flap frequency is reduced below $1.125/rev$. This peak vibration coincides with the second natural flap frequency passing through $3/rev$. With optimal $2/rev$ and $3/rev$ flap and lag stiffness variations (determined using gradient based optimization, with input constraint) vibration levels are reduced significantly over the entire range of flap frequency variation (vibration index, J_z , seen to be less than 8% in Fig. 8). The stiffness variation (input effort) required does not show great sensitivity to flap frequency variation (as seen by the fact that J_k remains relatively unchanged).

Figure 9 shows the hub vibration index, J_z , for variation in fundamental lag frequency. As the blade baseline lag stiffness, \overline{EI}_ζ , (and lag frequency) decreases, the vibration index (without cyclic stiffness variation) increases sharply when the first natural lag frequency is around $0.7/rev$. This sharp vibration peak occurs due to the second natural lag frequency passing through $4/rev$, and is exacerbated by the low damping in the lag mode. With optimal $2/rev$ and $3/rev$ flap and lag stiffness variations, it is seen in Fig. 9 that vibration levels are reduced significantly over the entire range of lag frequency variation (even around the aforementioned resonance). Furthermore, the stiffness variation (input effort) required does not show great sensitivity to lag frequency variation (J_k remains relatively uniform).

Figure 10 indicates that variation in the blade torsion stiffness, GJ , (corresponding to a torsion frequency variation between $3/rev$ and $5/rev$) does not produce any significant changes in baseline vibration index (in the absence of stiffness variations). With optimal $2/rev$ and $3/rev$ flap and lag stiffness variations, vibration levels are reduced by over 90%, over the entire range, with the stiffness variation (input effort) required, once again showing little sensitivity to torsion frequency variation (J_k relatively uniform).

4.5 Effectiveness of vibration controller at different forward speeds

This section examines the effectiveness of cyclic stiffness variations for vibration reduction at different forward speeds. Figure 11 shows the hub vibration index, J_z , over forward speeds ranging from advance ratio 0.25 to 0.35. It is seen that as the advance ratio increases, the baseline vibrations (without cyclic stiffness variation) increase dramatically; with the index J_z increasing from 30% to 275% of the value at advance ratio 0.3. However, with optimal $2/rev$ and $3/rev$ flap and lag stiffness variations (determined using gradient based optimization, with input constraint) the vibration index, J_z , is much smaller (well below 20%) and shows a much milder increase with advance ratio. It should be noted that in Fig. 11, the optimal stiffness variations are recomputed at different forward speeds. The input effort index, J_k , shows only a mild increase with advance ratio suggesting that there should be no actuator saturation problem at higher speeds.

4.6 Effect of Discrete Variable Stiffness Devices in Reducing Vibration

This section focuses on variable stiffness springs (representative of discrete controllable stiffness devices, Fig. 2), and demonstrates their effectiveness in reducing helicopter hub vibrations. It should be noted that the device introduced at the rotor hub would have both “steady” and “controllable” components of stiffness. The steady component could significantly change the baseline rotor configuration and the corresponding vibration levels, stresses, handling qualities, etc. For an accurate assessment of the effect of the cyclic stiffness variations of the device, the baseline configuration must be changed as little as possible. Thus, in the present study, when flap springs K_w and K_w' are introduced, the flap flexural stiffness of the root element is reduced to 70% of its baseline value. Similarly, when lag springs K_v , and K_v' are introduced, the lag flexural stiffness of the root element is reduced to 60% of its baseline value. The steady flap and lag spring stiffness values used in the simulations are given in Table 8, and these selections keep the rotor frequencies close to the baseline values (without introduction of discrete devices) as seen in Table 9.

Initially, only a controllable *flap* stiffness device is considered, and the optimal $3/rev$ stiffness variation to minimize the vibration performance index, J_z , is determined using gradient-based method. Figure 12 shows the reductions in hub vibration for the optimal $3/rev$ flap stiffness variation (amplitude $\Delta K_w^{3p} = 16\%$ of \overline{K}_w , and phase, $\phi = 0.8^\circ$). Reductions of over 50% are observed in the in-plane vibratory hub forces and the vibratory yaw moment. Smaller reductions of 10-35% are observed in the vibratory roll and pitch moments, respectively. The vibration performance

index, J_z , is reduced to 55% of the baseline value (implying a 45% reduction in the vibration index).

Finally, controllable stiffness devices are introduced in both the flap and lag directions, and optimal $2/rev$ and $3/rev$ stiffness variations are determined (using gradient-based approach) to minimize J_z . The optimal stiffness variations required are given in Table 10, and the corresponding vibration reductions are shown in Fig. 13. From the figure it is seen that approximately 55-70% reductions in vibratory hub forces, and 70% reduction in vibratory roll and pitch moments are achieved. A smaller reduction in vibratory yaw moment (under 20%) is also observed. The vibration performance index, J_z , is reduced to 13% of the baseline value.

The results in this section clearly demonstrate that optimal control of discrete variable stiffness devices would produce reductions in hub vibrations. It is anticipated that cyclic variation of blade root stiffness would be practically accomplished through the introduction of such discrete controllable stiffness elements.

5. Concluding Remarks

In the present study it is demonstrated that optimal multi-cyclic variation of blade root flap and lag stiffness can produce simultaneous reductions in all components of vibratory hub loads of a 4-bladed BO-105 type hingeless rotor helicopter. Both gradient and non-gradient based optimization schemes were successful in reducing the hub vibrations. Further, the required stiffness variations could be reduced (without significantly compromising performance) by introducing a penalty on the input in the objective function used for minimization. Reductions in the vibration performance index of over 90% were seen with optimal $2/rev$ and $3/rev$ flap and lag stiffness variations.

Multi-cyclic flap and lag stiffness variations were seen to be effective in reducing hub vibration even when the fundamental rotor properties (such as fundamental flap, lag, and torsion frequencies) were changed. Similarly, the concept was effective in reducing vibration at various forward speeds, without significant change in the required stiffness variation inputs.

The paper also demonstrates that cyclic variations in the stiffness of *discrete flap and lag springs* introduced in the blade root region are effective in reducing vibratory hub loads. Cyclic variation of properties of discrete controllable devices effectively varies the stiffness of the blade root region, and this constitutes a viable method for practical implementation.

References

- 1 Reichert, G., "Helicopter Vibration Control – Survey," *Vertica*, Vol. 5, No. 1, 1981, pp. 1-20.
- 2 Lowey, R. G., "Helicopter Vibrations: A Technological Perspective," *Journal of the American Helicopter Society*, Vol. 29, No. 4, Oct. 1984, pp. 4-30.
- 3 Nguyen, K., "Higher Harmonic Control Analysis for Vibration Reduction of Helicopter Rotor Systems," Ph.D. Thesis, University of Maryland, 1989.
- 4 Milgram, J. H. and Chopra, I., "A Parametric Design Study for Actively Controlled Trailing Edge Flaps," *Journal of the American Helicopter Society*, Vol. 43, No. 2, April 1998, pp. 110-119.
- 5 Welsh, W., Fredrickson, C., Rauch, C., and Lyndon, I., "Flight Test of An Active Vibration Control System on the UH-60 Black Hawk Helicopter," *Proceedings of the American Helicopter Society 51st Annual Forum*, May 1995, pp. 393-402.
- 6 Staple, A. E., "An Evaluation of Active Control of Structural Response as a Means of Reducing Helicopter Vibration," *Proceedings of the 15th European Rotorcraft Forum*, Amsterdam, Netherlands, September 1989, pp. 51.1-51.18.
- 7 Ganguli, R. and Chopra, I., "Aeroelastic optimization of an Advanced Geometry Helicopter Rotor," *Journal of the American Helicopter Society*, Vol. 41, No. 1, January 1996, pp. 18-28.
- 8 Chen, P. and Chopra, I., "Induced Strain Actuation of Composite beams and Rotor Blades with Embedded Piezoceramic elements," *Proceedings of the SPIE on Smart Structures and Materials*, 1994.
- 9 Jacklin, S. A., Blaas, A., Teves, D., and Kube, R., "Reduction of Helicopter BVI Noise, Vibration and Power Consumption through Individual Blade Control," *Proc. of the American Helicopter Society 51st Annual Forum*, May 1995, pp. 662-680.
- 10 Shaw, J. et. al., "Higher Harmonic Control: Wind Tunnel Demonstration of Fully Effective Vibratory Hub Force Suppression," *Journal of the American Helicopter Society*, Vol. 34, No. 1, January 1989.
- 11 Anusonti-Inthra, P., and Gandhi, F., "Helicopter Vibration Reduction through Cyclic Variations in Rotor Blade Root Stiffness," *Proceedings of the American Helicopter Society 55th Annual Forum*, Montreal, Canada, May 1999.
- 12 Yang, J. N., Wu, J. C., and Li, Z., "Control of Seismic-excited Buildings using Active Variable Stiffness Systems," *Engineering Structures*, Vol. 19, No. 9, 1996, pp. 589-596.
- 13 Patten, W. N., Mo, C., Kuehn, J., and Lee, J., "A Primer on Design of Semiactive Vibration Absorbers (SAVA)," *Journal of Engineering Mechanics*, Vol. 124, No. 1, January 1998, pp. 61-68.
- 14 Sadek, F. and Mohraz, B., "Semiactive Control Algorithms for Structures with Variable Dampers,"

- Journal of Engineering Mechanics*, Vol. 124, No. 9, September 1998, pp. 981-990.
- 15 Gavin, H. P. and Doke, N. S., "Resonance Suppression through Variable Stiffness and Damping Mechanisms," *Proceedings of the SPIE Smart Structures Conference*, SPIE Vol. 3671, March 1999, pp 43-53.
 - 16 Krasnicki, E. J., "Comparison of Analytical and Experimental Results for a Semi-Active Vibration Isolator," *The Shock and Vibration Bulletin*, The Shock and Vibration Information Center, Naval Research Laboratory, Vol. 50. 1980.
 - 17 Krasnicki, E. J., "The Experimental Performance of an Off-Road Vehicle Utilizing a Semi-Active Suspension," *The Shock and Vibration Bulletin*, The Shock and Vibration Information Center, Naval Research Laboratory, 1984.
 - 18 Hrovat, D., Margolis, D. L., and Hubbard, M., "An Approach Toward the Optimal Semi-Active Suspension," *Journal of Dynamic Systems, Measurement and Control*, Vol. 110, September 1988, pp. 288-296.
 - 19 Karnopp, D., "Design Principles for Vibration Control Using Semi-Active Dampers," *Journal of Dynamic Systems, Measurement and Control*, Vol. 112, September 1990, pp. 448-455.
 - 20 Symans, M. D. and Constantinou, M. C., "Semi-active Control Systems for Seismic Protection of Structures: A State-of-the-art review," *Engineering Structures*, Vol. 21, 1999, pp. 469-487.
 - 21 Marathe, S., Gandhi, F., and Wang, K. W., "Helicopter Blade Response and Aeromechanical Stability with a Magnetorheological Fluid Based Lag Damper," *Journal of Intelligent Material Systems and Structures*, Vol. 9, No. 4, April 1998, pp. 272-282.
 - 22 Kamath, G. M., Wereley, N. M., and Jolly, M. R., "Characterization of Magnetorheological Helicopter Lag Dampers," *Journal of the American Helicopter Society*, Vol. 44, No. 3, July 1999, pp. 234-248.
 - 23 Bir, G., Chopra, I., *et al*, "University of Maryland Advanced Rotorcraft Code (UMARC) Theory Manual," UM-AERO Report 92-02, Aug. 1992.
 - 24 Johnson, W., "Self-tuning regulators for multicyclic control of helicopter vibration," NASA Technical Paper 1996, March 1982.
 - 25 Carroll, D. L., "Fortran Genetic Algorithm Driver version 1.7," Talbot Lab, University of Illinois, Urbana, Illinois, Dec 1998.

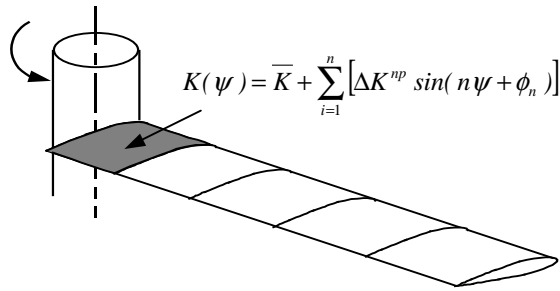


Figure 1: Discretized rotor blade

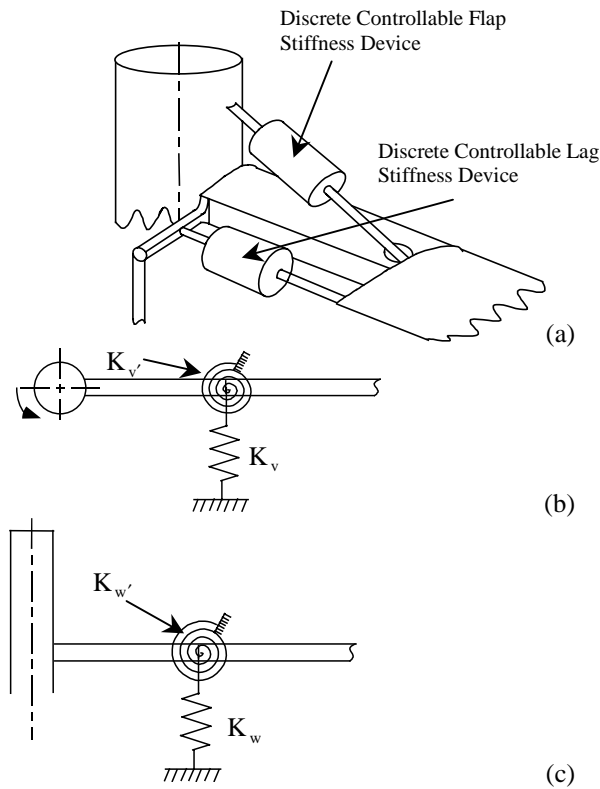


Figure 2: (a) Sketches of discrete controllable stiffness elements and their mathematical idealization in (b) lead-lag and (c) flap direction.

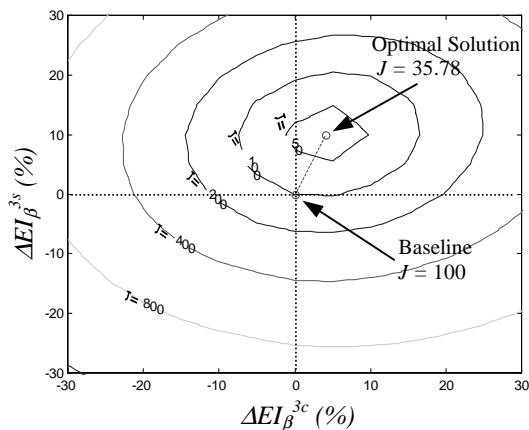


Figure 3: Contour plot of performance index, J , (% Baseline) due to 3/rev flap stiffness variations

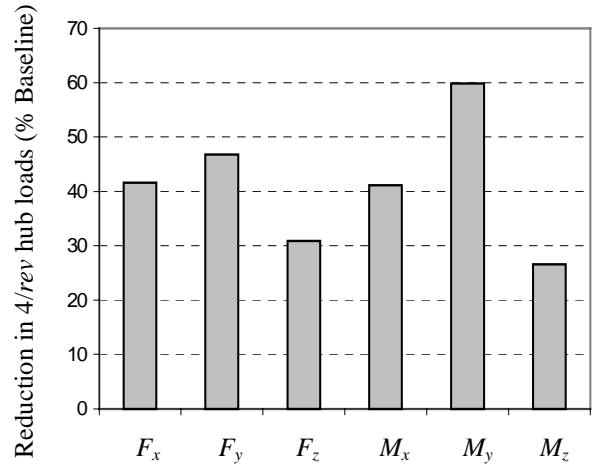


Figure 4: Hub vibration reduction due to optimal 3/rev flap stiffness variation

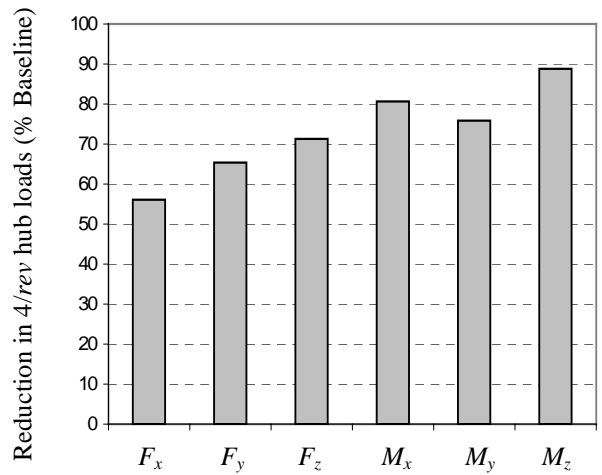


Figure 5: Hub vibration reduction due to optimal 2,3/rev flap and 3/rev lag stiffness variations

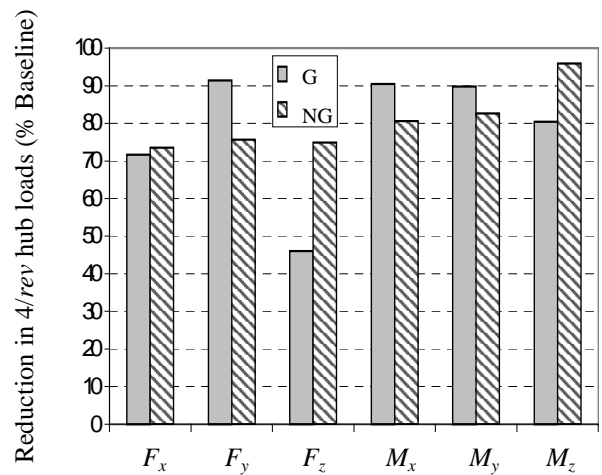


Figure 6: Hub vibration reduction due to optimal 2,3/rev flap and lag stiffness variations with gradient based (G) and non-gradient based (NG) approach

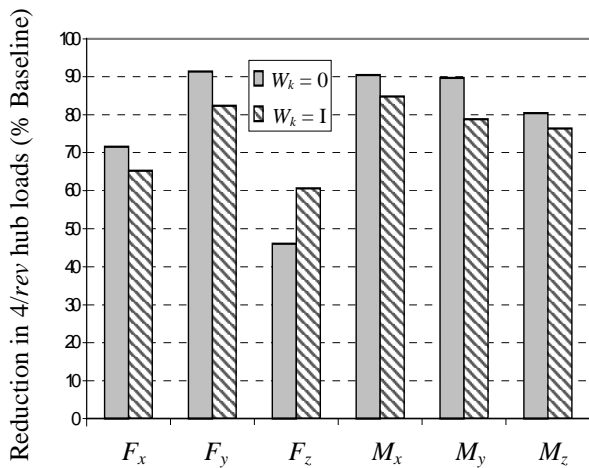


Figure 7: Hub vibration reduction due to optimal 2,3/rev flap and lag stiffness variations with ($W_k = 1$) and without ($W_k = 0$) input constraint

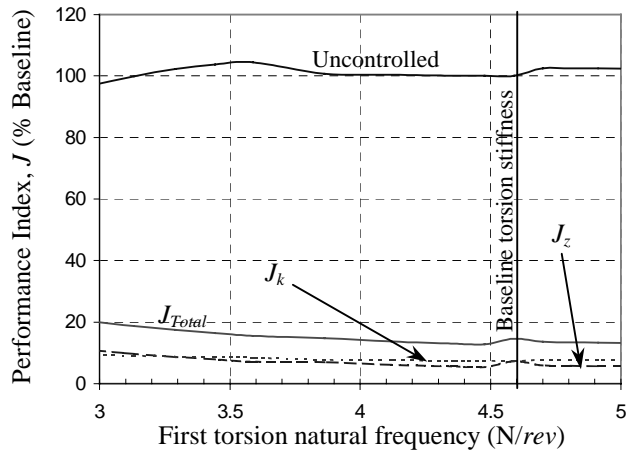


Figure 10: Effectiveness of optimal 2,3/rev flap and lag stiffness variations for different values of torsion stiffness of the blade

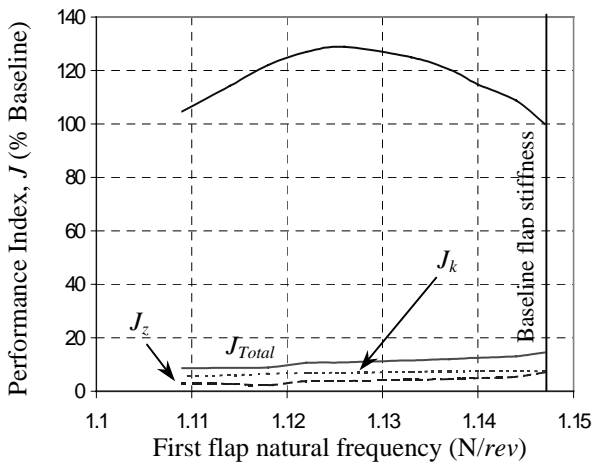


Figure 8: Effectiveness of optimal 2,3/rev flap and lag stiffness variations for different values of steady flap stiffness of the blade

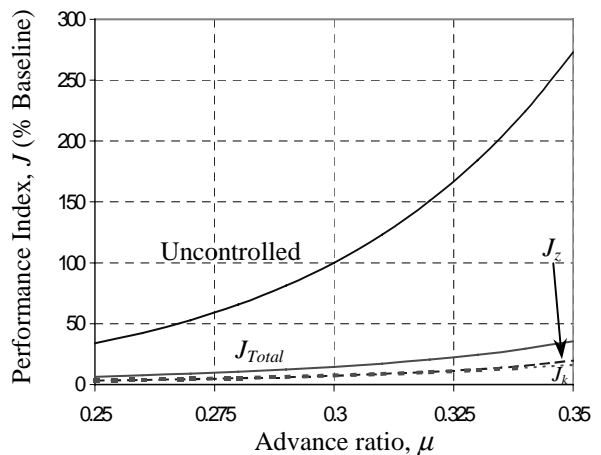


Figure 11: Effectiveness of optimal 2,3/rev flap and lag stiffness variations for different advance ratios

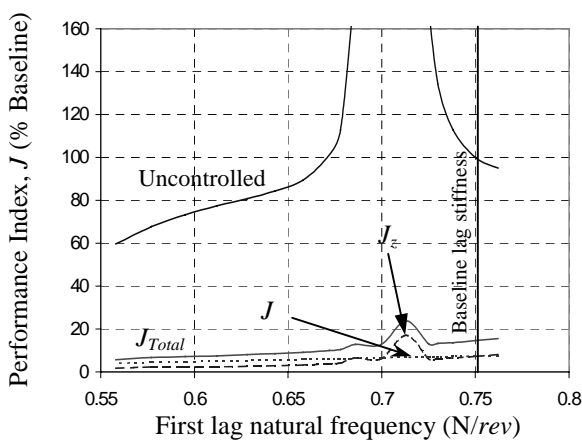


Figure 9: Effectiveness of optimal 2,3/rev flap and lag stiffness variations for different values of steady lag stiffness of the blade

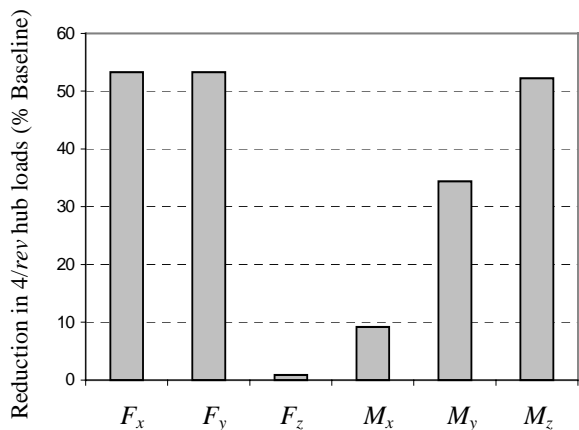


Figure 12: Hub vibration reduction due to optimal 3/rev stiffness variation of discrete flap springs

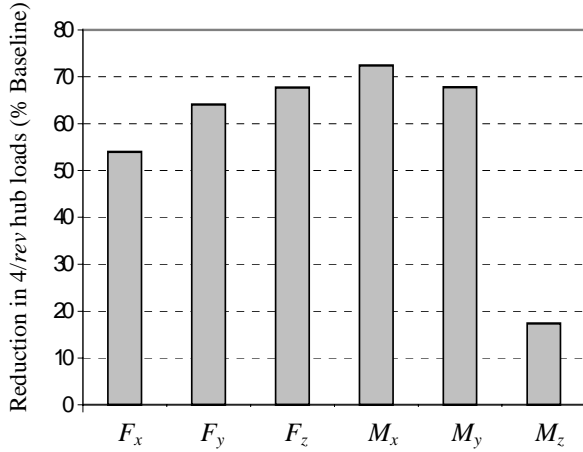


Figure 13: Hub vibration reduction due to optimal 2,3/rev stiffness variations of discrete flap and lag springs

Main Rotor Properties	Number of blades	4
	Lock number, γ	6.34
	Solidity ratio, σ	0.1
	Rotational speed, Ω (Rad./s)	40.1234 rad/s
	C_T/σ	0.07
Rotor Blade Properties	Blade radius, R	16.2 ft.
	Blade chord, c/R	0.08
	Mass per unit length, m_o	0.135 slug/ft
	Flap bending stiffness $EI_\beta/m_o\Omega^2R^4$	0.008345
	Lag bending stiffness $EI_\zeta/m_o\Omega^2R^4$	0.023198
	Torsional stiffness $GJ/m_o\Omega^2R^4$	0.003822
	Lift curve slope, a	5.73
	Skin friction drag coefficient, C_{d0}	0.0095
	Induced drag coefficient, C_{d2}	0.2
	Pitching moment coefficient, C_m	0.0
Tail Rotor Properties	Number of blades, N_{tr}	4
	Tail rotor radius, R_{tr}	3.24 ft.
	Solidity ratio, σ_{tr}	0.15
	Rotor speed, Ω_{tr}	5Ω
	Lift curve slope, a_{tr}	6.0
	Tail rotor location, $(x_{tr}/R, z_{tr}/R)$	(1.2, 0.2)
Horizontal Tail Properties	Horizontal tail area, $S_{ht}/\pi R^2$	0.011
	Horizontal tail lift curve slope, a_{ht}	6.0
	Horizontal tail location, x_{ht}/R	0.95
Fuselage Properties	C.G. location, (x_{cg}, y_{cg})	(0, 0)
	Hub location, h/R	0.2
	Net weight, W	5800 Lbs.

Table-1: Rotor and fuselage properties

Hub Loads	Baseline Values (Non-dimensional*)
F_x^{4p}	0.010937
F_y^{4p}	0.010910
F_z^{4p}	0.007258
M_x^{4p}	0.083085
M_y^{4p}	0.086632
M_z^{4p}	0.065129

*Non-dimensional factors are F_z^0 (5940 lbs.) for all hub forces and M_z^0 (5244.5 ft-lbs.) for all hub moments

Table-2a: 4/rev vibratory hub loads for baseline rotor (no stiffness variation), $\mu = 0.3$

Blade Root Loads	Baseline Values (Non-dimensional*)				
	1/rev	2/rev	3/rev	4/rev	5/rev
S_r	0.085114	0.008036	0.003606	0.001891	0.000092
S_x	0.072238	0.003599	0.001990	0.004815	0.000240
S_z	0.053513	0.039237	0.015058	0.001815	0.000483
M_ϕ	0.012710	0.004204	0.000335	0.000176	0.000029
M_β	0.192777	0.124387	0.042688	0.004195	0.001321
M_ζ	0.384243	0.018488	0.004317	0.016282	0.000898

*Non-dimensional factors are F_z^0 for all forces and M_z^0 for all moments

Table-2b: Harmonics of blade root loads for baseline rotor (no stiffness variation), $\mu = 0.3$

	1p	2p	3p	4p	5p
S_r	-0.03	-3.35	-19.73	24.45	-38.55
S_x	-0.12	-2.13	-62.01	-17.08	-33.41
S_z	0.70	-1.94	-61.32	-30.92	59.58
M_ϕ	0.09	-1.20	-12.75	-27.71	-14.74
M_β	-0.02	-3.83	-50.76	11.19	231.91
M_ζ	-0.11	4.72	-55.01	-26.62	-3.01

Table 3: Percentage change in harmonic of blade root loads due to optimal 3/rev flap stiffness variation

J_z	Input	2/rev		3/rev	
		Amp	Phase	Amp	Phase
8.92	ΔEI_β	23	-111°	15	31°
	ΔEI_ζ	--	--	8	42°

Table 4: Performance index and optimal 2,3/rev flap and 3/rev lag stiffness variations

	J_z	Input	2/rev		3/rev	
			Amp	Phase	Amp	Phase
G	7.34	ΔEI_β	22	-102°	14	48°
		ΔEI_ζ	31	45°	8	47°
NG	3.55	ΔEI_β	23	-125°	14	27°
		ΔEI_ζ	9	66°	7	41°

Table 5: Performance index and optimal 2,3/rev flap and lag stiffness variations for gradient based (G) and non-gradient based (NG) optimization

W_k	Input	2/rev		3/rev	
		Amp	Phase	Amp	Phase
0	ΔEI_β	22	-102°	14	48°
	ΔEI_ζ	31	45°	8	47°
I	ΔEI_β	18	-108°	13	37°
	ΔEI_ζ	15	59°	6	44°

Table 6: Optimal 2,3/rev flap and lag stiffness variations with ($W_k = I$) and without ($W_k = 0$) input constraint

	1p	2p	3p	4p	5p
S_r	1.62	-11.57	-34.60	-65.57	160.51
S_x	2.04	0.77	-22.39	-86.37	194.45
S_z	1.75	5.60	-26.26	-60.63	77.53
M_ϕ	0.58	-2.06	-50.34	112.65	66.93
M_β	-0.28	43.44	-83.15	25.06	167.71
M_ζ	2.12	-18.61	40.85	-76.33	254.16

Table 7: Percentage change in harmonic of blade root loads due to the optimal 2,3/rev flap and lag stiffness variations ($W_k = I$)

\bar{K}_w	$0.2 \bar{EI}_\beta / R^3$
$\bar{K}_{w'}$	$0.2 \bar{EI}_\beta / R$
\bar{K}_v	$0.1 \bar{EI}_\zeta / R^3$
$\bar{K}_{v'}$	$0.1 \bar{EI}_\zeta / R$

Table 8: Equivalent flap and lag spring stiffness of discrete stiffness device

Mode		Baseline (/rev)	With discrete devices (/rev)
Flap	1 st	1.147	1.199
	2 nd	3.405	3.593
	3 rd	7.508	7.825
Lag	1 st	0.75	0.802
	2 nd	4.372	4.503
	3 rd	11.073	11.174
Torsion	1 st	4.59	4.59
	2 nd	13.601	13.601

Table 9: Comparison of rotor natural frequencies for rotor systems with and without discrete stiffness devices

J_z	Input	2/rev		3/rev	
		Amp	Phase	Amp	Phase
13.1	ΔK_w	21	-102.5°	21	35.2°
	ΔK_v	9	107.0°	4	16.5°

Table 10: Performance index and optimal 2,3/rev stiffness variations of discrete flap and lag springs